C. R. Chimie 18 (2015) 1264–1269

Contents lists available at ScienceDirect

Comptes Rendus Chimie

www.sciencedirect.com

Full paper/Mémoire

Hydrogenation of CO_2 into hydrocarbons over bifunctional system Cu–ZnO/Al_2O_3 + HZSM-5: Effect of proximity between the acidic and methanol synthesis sites

Hydrogénation du CO_2 en hydrocarbures sur des catalyseurs bifonctionnels Cu–ZnO/Al_2O_3 + HZSM-5 : effet de la proximité entre les sites acides et les sites métalliques de synthèse du méthanol

Hania Ahouari [a], Ahcène Soualah [a,*], Anthony Le Valant [b], Ludovic Pinard [b], Yannick Pouilloux [b]

[a] *Laboratoire de physicochimie des matériaux et catalyse, Faculté des sciences exactes, Université de Bejaia, 06000 Bejaia, Algeria*
[b] *IC2MP, UMR 7285 CNRS, Université de Poitiers, 86022 Poitiers cedex, France*

ARTICLE INFO

Article history:
Received 13 April 2015
Accepted after revision 21 July 2015
Available online 12 September 2015

Keywords:
CO_2
Bifunctional catalysts
Hydrocarbons synthesis
Oxide–zeolite proximity

Mots clés :
CO_2
Catalyseurs bifonctionnels
Synthèse des hydrocarbures
Proximité oxyde–zéolithe

ABSTRACT

A one-step CO_2 hydrogenation reaction into hydrocarbons (HC) using a bifunctional system constituted by a methanol synthesis catalyst [Cu–ZnO–Al_2O_3 (CZA)] and a zeolite (HZSM-5) has been studied. The influence of the catalyst bed configuration on activity, selectivity, and HC yield has been evaluated. The results obtained at T_R = 623 K, P_R = 3.0 MPa and WHSV = 6000 h^{-1} show that CO_2 hydrogenation and hydrocarbon selectivity were strongly influenced by the proximity between oxide and zeolite, whatever the disposition of the two catalytic active sites. Indeed, the highest conversion and the best yield of hydrocarbons (mainly C_2) were obtained with the M1 bifunctional catalysts in which the oxide–zeolite proximity is the lowest. This is ascribed to the hydrogen spillover phenomenon, which does not promote the carbon chain growth.

RÉSUMÉ

L'hydrogénation catalytique du CO_2 en hydrocarbures (HC) sur des catalyseurs bifonctionnels préparés par mélange physique d'un catalyseur de synthèse du méthanol Cu–ZnO–Al_2O_3 (CZA) et d'une zéolithe HZSM-5 a été étudiée. L'influence de la proximité oxyde–zéolithe sur l'activité, la sélectivité et le rendement en hydrocarbures ont été évalués. Les résultats obtenus pour T_R = 623 K, P_R = 3,0 MPa and WHSV = 6000 h^{-1} montrent que l'hydrogénation du CO_2 et la sélectivité en hydrocarbures sont fortement influencées par la proximité entre l'oxyde et la zéolite, quelle que soit la disposition des deux sites actifs. En effet, la conversion la plus élevée et le meilleur rendement en hydrocarbures (principalement C_2) ont été obtenus avec la plus faible proximité oxyde–zéolithe. Cela est dû au phénomène d'hydrogène épandu, qui ne favorise pas la croissance de la chaîne carbonée.

* Corresponding author.
E-mail address: soualah.ahcene@yahoo.fr (A. Soualah).

http://dx.doi.org/10.1016/j.crci.2015.07.005
1631-0748/

1. Introduction

The increase in the environmental impact of a high CO_2 concentration on the atmosphere through the greenhouse effect has been of acute concern to the global community. Many efforts have been made to reduce CO_2 emissions and to improve the climate conditions using various procedures such as removal, recovery, and storage [1–8]. However, it is desirable to develop a technique whereby carbon dioxide recovered can be converted into valuable materials [2,3]. Therefore, catalytic conversion of CO_2 into useful chemicals like methanol or hydrocarbons is one of the efficient ways not only to curtail the growing amount of carbon dioxide emission, but also to improve economic benefits [1,6,9–11]. Notwithstanding an extensive literature concerning the production of hydrocarbons via syngas hydrogenation [8–19], only few papers deal with hydrocarbons synthesis via CO_2 hydrogenation [5,20–29].

Fundamentally, there are two routes for the production of hydrocarbons through CO_2 hydrogenation:

- a two-step process, in which methanol is initially produced in the first reactor over a metallic catalyst site, followed by methanol conversion into hydrocarbons via DME according to an MTG or MTO process over the acid catalyst located in a second reactor [2,3,14,15];
- a one-step process, in which a bifunctional catalyst prepared by physically mixing metallic and acidic functionalities are used in only one reactor [30–32].

Methanol is initially produced on a metallic catalyst and then dehydrated into DME on an acidic site of the zeolite. Thus, the DME formed in turn is converted into ethene and then higher into hydrocarbons through oligomerization and isomerization reactions [17]. After that, ethene or other alkenes, which are transported to the metallic catalyst, are hydrogenated into the corresponding alkanes, preventing carbon homologation and restraining the formation of heavier hydrocarbons [17]. Fujimoto and Shikada [2] claimed that the hydrogenation of alkene by the metallic catalyst plays an important role in hydrocarbon synthesis through CO_2 hydrogenation.

The main advantage of the single-step process is the elimination of the thermodynamic restriction of methanol synthesis.

We can assume that the transport step between the metallic and the acidic sites of the bifunctional catalysts plays a significant role in the catalytic performances and in the hydrocarbons' selectivity (see Fig. 1).

Catalysts for the direct CO_2-to-HC process should be able to efficiently catalyze both methanol and hydrocarbon synthesis reactions, while the yield of CO formed via the RWGS side reaction [27] should be kept low and/or be transformed into methanol. Typically, the methanol synthesis reaction is carried out on Cu–ZnO–Al_2O_3 catalysts, while the hydrocarbon reaction occurs mainly over a solid acid component, as a zeolite.

Indeed, our challenge in this study is to achieve CO_2 hydrogenation into hydrocarbons in a one-step process using a bifunctional system constituted by a methanol synthesis catalyst, Cu–ZnO–Al_2O_3 (CZA), and a zeolite (HZSM-5).

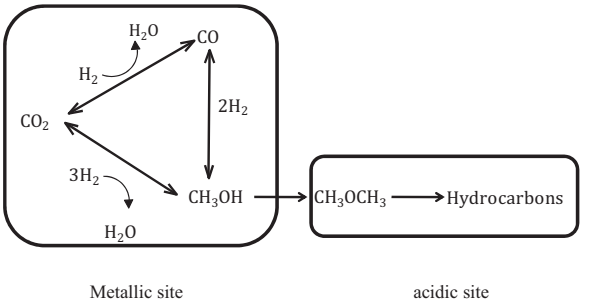

Fig. 1. CO_2 hydrogenation into hydrocarbons in one single step using a bifunctional system.

In order to evaluate the effect of the proximity between metallic and acidic sites on CO_2 activation, hydrogenation and methanol dehydration into hydrocarbons, three different combination dispositions of the two components have been adopted.

2. Experimental

2.1. Catalyst preparation

A copper-based catalyst Cu–ZnO–Al_2O_3 (CZA) with nominal composition Cu:Zn:Al = 51.0:22.0:3.5 wt. %, determined by ICP-AES, was prepared according to a procedure described in detail elsewhere [30].

To evaluate the effect of the contact between the two catalytic functions, metallic-acid sites, on hydrocarbons synthesis, the copper-based catalyst CZA was admixed to a commercial HZSM-5 microporous zeolite (Zeolyst Int.CBV3024E). The physicochemical properties of the acidic catalysts (HZSM-5) are listed below: framework Si/Al ratio = 40, surface area = 452 $m^2 \cdot g^{-1}$, pore volume = 0.3 $cm^3 \cdot g^{-1}$. The acidity of the zeolite (number of Brønsted acid sites able to retain pyridine at 150 °C, infrared spectroscopy) was 297 $\mu mol \cdot g^{-1}$.

Three different dispositions of the metallic and the acidic catalysts (see Fig. 2) adopted during the catalytic tests are described in details in the following section:

- M1 is used to load the two catalysts in a dual-bed arrangement; the contact between the catalysts was avoided by a glass wool between the catalysts layers;

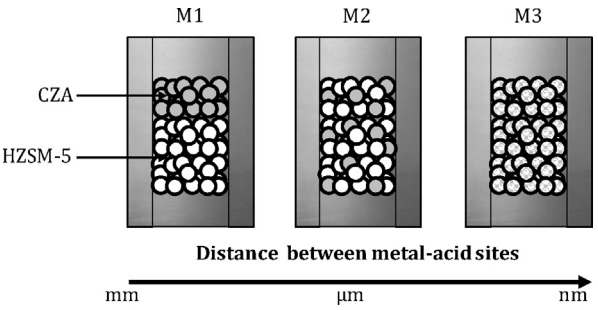

Fig. 2. Combination procedures between methanol and acid catalysts [●: Cu–ZnO–Al_2O_3 (CZA); ○: a zeolite (HZSM-5)].

- M2 is used to grind, pressure mold, crush and sieve each component CZA and HZSM-5, respectively, to prepare particles of 0.2–0.4 mm. Then, the particles of each component were thoroughly mixed;
- M3 is to grind the fine particles of CZA and HZSM-5 catalysts in a porcelain mortar for sufficient time so that the two kinds of catalysts could be further uniformly mixed and then the mixture is pelletized, crushed, and sieved until a 0.2–0.4-mm particle size.

Considering the results obtained previously in our laboratory dealing with the effect of zeolite loading within the hybrid catalyst on the activity and the yield of hydrocarbons, a weight ratio of 1/3 (oxide/zeolite) was used to prepare the different dispositions.

2.2. Characterization of the catalysts

2.2.1. Nitrogen adsorption–desorption (BET)

The surface areas of the oxide, hybrid and HZSM-5 catalysts were determined by adsorption–desorption of nitrogen at the temperature of liquid nitrogen (−196 °C) using a Micromeritics Tristar and ASAP 2000 instruments. Before measuring, the samples (oxide and hybrids) were degassed at 250 °C for 4 h and the zeolite HZSM-5 was heated at 350 °C overnight. The surface areas were calculated according to the method of Brunauer, Emmet and Teller (BET).

2.2.2. In situ *X-ray diffraction*

In situ XRD measurements were collected using an ADVANCE D8 diffractometer with a Cu Kα radiation source (λ_1 = 1.54056 Å, λ_2 = 1.54439 Å) equipped with a high-temperature reaction cell to enable the temperature-driven *in situ* reduction of the catalysts.

The catalysts were exposed to 3%H_2/He at 30 °C for 1 h and then the temperature of the oven was raised from 50 to 350 °C at a rate of 5 °C/min.

The sample was kept 1 h in a reducing atmosphere at each temperature, except at 350 °C, at which it was kept for 4 h. The diffraction pattern was recorded every 50 °C in the 2θ range from 20° to 90° with a step size of 0.024° and a time/step of 1 s.

After subtraction of the background and correction for instrumental broadening, the peak width and the diffraction angle 2θ were used to calculate the average crystallite size d_{hkl} [18]:

$$d_{hkl} = \frac{0.94\lambda}{\beta(2\theta)\cos\theta}$$

where λ is the X-ray wavelength, and $\beta(2\theta)$ the full width at half-maximum, in radians.

2.2.3. H_2 adsorption

Hydrogen adsorption measurements were performed at 30 °C using a Micromeritics Autochem 2920II apparatus. The samples were reduced for 3 h at 350 °C in a hydrogen flow (30 mL/min), which was subsequently evacuated using an argon flow (30 mL/min) at the same temperature for 1 h. The reactor was cooled down to room temperature using argon and then pulses of 10% H_2/Ar were injected until saturation. After that, the sample was degassed with argon for 10 min to evacuate the H_2 physisorbed, which was followed by another series of H_2 pulse injections.

2.3. Catalytic testing

Carbone dioxide hydrogenation was performed in a continuous-flow fixed-bed reactor (12.5 mm id) made of stainless steel, using 0.5 g of oxide catalyst or 2 g of hybrid catalyst, diluted with silicon carbide to avoid thermal effects (hot spots) (SiC, d = 1.9 mm) at a weight ratio of 4:1. The temperature in the tubular reactor was controlled with a coaxially centered thermocouple in contact with the catalytic bed.

The catalysts used in this reaction were loaded in the reactor according to the three ways presented in Fig. 2. Prior to the reaction, the sample was reduced *in situ* at 350 °C at a heating rate of 5 °C/min under a flow of H_2 (30 mL/min, 99.99% H_2) for 4 h at atmospheric pressure. After that, a gas mixture (H_2/CO_2 = 3) was introduced into the reactor at 350 °C, and the pressure was then raised up to 3.0 MPa. The liquid products were separated from the gas flow in the gas liquid separator and the condenser. The effluent products from the heated line were analyzed by an online gas chromatograph system, which was composed of three gas chromatographs:

- Porapak Q, TCD for CO and CO_2;
- AT-Aquawax (FID) for methanol and dimethylether (CH_3OH, CH_3OCH_3);
- with a capillary column HP-Plot Q, FID for hydrocarbons (C_1-C_6).

All analysis lines and valves were heated at 150 °C to prevent a possible condensation of the products before entering the gas chromatograph.

3. Results and discussion

3.1. XRD diffraction

In situ XRD powder patterns recorded for different temperatures of the hybrid catalyst M3 are shown in Fig. 3. The presence of alumina and HZSM-5 phases in the hybrid catalyst is clearly confirmed by the Bragg diffraction peaks at 2θ = 44.4° (JCPDS 34-0493) for alumina and at 23–25° for HZSM-5, whatever the temperature. However, heating the sample between RT and 200 °C does not induce changes in the crystal structure, and the XRD powder patterns are fully indexed using mainly two phases: CuO at 2θ = 35°, 38.8° (JCPDS 00-045-0937) and to ZnO at 2θ = 31°, 36° (JCPDS 00-036-1451).

Beyond 200 °C and up to 350 °C, we noticed a full disappearance of the peaks relative to copper oxide CuO at the expense of new peaks related to metallic copper peaks at 2θ = 43.3°, 50° and 73° (JCPDS 01-089-2838), which indicates a complete reduction of CuO into Cu. However, no changes were observed for zinc oxide and the peaks

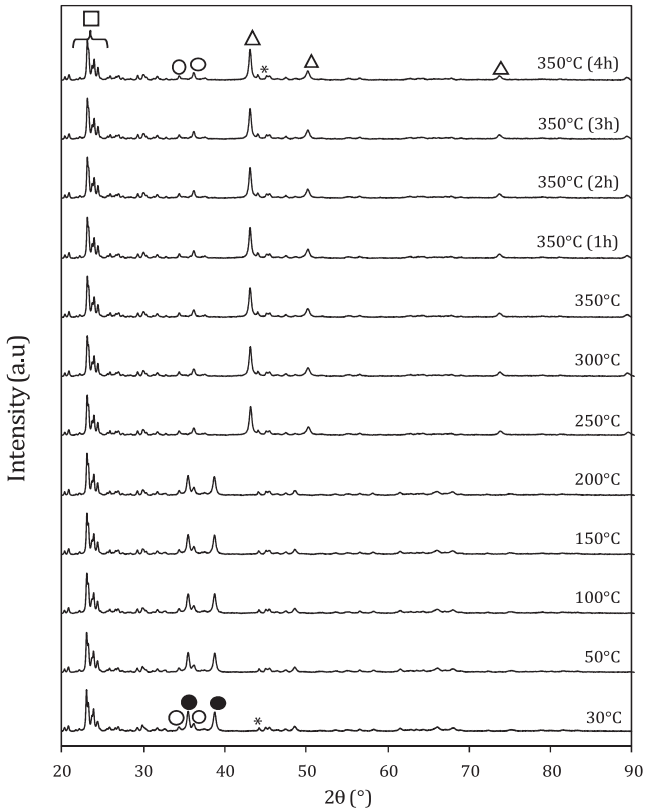

Fig. 3. *In situ* X-ray diffraction patterns of hybrid catalyst (M3) recorded during reduction in 3% H_2 in He. ●: CuO; ○: ZnO; △: Cu; ⁎: Al_2O_3; □: a zeolite (HZSM-5).

relative to ZnO are still remaining in the structure. The particle sizes of CuO and Cu in the oxide and the hybrid catalysts determined using the Scherrer equation are 28 nm and 34 nm, respectively. This result means that the addition of zeolite had no effect on the particle size (Table 1).

Table 1
CuO and Cu particles size of the catalysts.

Catalyst	*d* (nm)[a]	
	Before reduction (CuO, 38.8°)	After reduction (Cu, 43°)
CZA	28	34
M3	28	34

CZA: Cu–ZnO–Al_2O_3.
[a] Particle sizes determined by the Scherrer equation.

3.2. Catalytic results

Carbon dioxide hydrogenation over oxide and hybrid catalysts were carried out using a stainless steel reactor under the following reaction conditions: $H_2/CO_2 = 3$, $T = 350$ °C, and $P = 3.0$ MPa; the results are listed in Table 2.

As shown in Table 2, carbon monoxide CO is the main product formed over the copper-based catalyst according to the reverse water gas shift reaction widely known from the literature. The high yield of carbon monoxide can be also attributed to methanol decomposition at high-temperature, as already reported in the literature [31], and this explains the small yield of MEOH formed at 350 °C (0.7%). A small amount of hydrocarbons was also detected (mainly CH_4 and C_2H_6). Over the hybrid catalysts, CO

Table 2
Effect of the contact between oxide and zeolite on carbon dioxide hydrogenation over the hybrid catalysts.

Test	CO_2 conv. (%)	Yield (%, C-mol)			O/(O + P)[b]	Coke (%)
		CO	MeOH	HC[a]		
MeOH synthesis[c]	30.3	29.6	0.7	–	–	–
CZA	32.0	29.0	2.4	0.6	0.0	0.4
CZA + HZSM5(M1)	36.4	24.6	0.0	11.8	1.0	1.8
CZA + HZSM5(M2)	37.3	21.6	0.3	15.3	0.1	1.2
CZA + HZSM5(M3)	39.8	21.3	1.6	16.8	0.0	0.5

Conv.: conversion; O: Olefins; P: Paraffin; CZA: Cu–ZnO–Al_2O_3; HZSM-5: a zeolite. Reaction conditions: 700 min, 350 °C, 3.0 MPa, GHSV = 6000 h^{-1}.
[a] O/(O + P) = C mol (olefin C_2 to C_6)/[(olefin C_2 to C_6) + (paraffin C_2 to C_6)].
[b] HC: hydrocarbons.
[c] Thermodynamic equilibrium.

remains predominant together with the formation of a good yield of hydrocarbons. In fact, mixing HZSM-5 with methanol synthesis catalysts improves significantly CO_2 conversion and the yield of hydrocarbons. The formation of hydrocarbons is explained by the transformation of methanol and dimethylether intermediates formed over copper-based catalysts into hydrocarbons over zeolite acid sites.

The proximity between the metallic and the acidic sites is one of the main keys in the formation of hydrocarbons through CO_2 hydrogenation. In fact, the investigation of the effect of the contact between the two catalytic functions on the hydrocarbons distribution and the selectivity is an important factor to be studied. This can bring a lot of clarifications on the mechanism of hydrocarbons formation over the hybrid catalysts. We plotted in Fig. 4 the hydrocarbons selectivity versus the number of carbons for the different catalytic bed arrangements.

Whatever the proximity between metallic and acidic sites (M1, M2 or M3), the selectivity to methane over the hybrid catalysts was low, and the distribution of hydrocarbons was shifted toward higher carbon numbers, selectively C_2. This behavior is pronounced with the increase of the proximity between oxide and zeolite, and the same results were previously reported by Jeon et al. [16]. According to them, the formation of ethane appears to be due to the abundance of strong Brønsted acid sites that have a high hydrogenating ability to reduce alkenes into alkanes.

The product distribution over the follow-bed arrangement (M1) and the single-bed system (M2) are quite similar. We can assume that the equilibrium constraints of methanol formation can be avoided by the removal of methanol from the gas phase through its conversion into hydrocarbons when the hybrid catalyst in the single-bed system (M2) is used. This equilibrium shift in the methanol synthesis mechanism enables a larger yield of hydrocarbons than the thermodynamically limited methanol formation from carbon dioxide. However, in the follow-bed arrangement (M1), the methanol formed over the copper catalyst in the first stage was converted into hydrocarbons over HZSM-5 in the second stage. The thermodynamic limits of methanol formation could not be overcome in this arrangement and the distribution of hydrocarbons follows the non-Anderson–Schultz–Flory distribution.

These results, therefore, indicate that, in the case of the composite catalysts, C_2^+ hydrocarbons were not formed directly from carbon dioxide, but through a MTG reaction of methanol obtained from carbon dioxide. The yields of C_4^+ hydrocarbons were extremely poor, and alkenes such as ethene and propene were not produced. The formation of higher hydrocarbons (C_4^+) is enhanced while decreasing the proximity between the two catalysts (oxide–zeolite), and the highest yield is obtained with the two-bed arrangements (M1). These results may be explained by hydrogen spillover, which does not promote the chain growth and the formation of heavier hydrocarbons. Consequently, the carbon deposit was lower on the hybrid catalysts loaded in the single-bed system compared to the duel bed arrangements, as we can see in Table 2. The same explanation has been already used by several researchers [29,32,33] and, according to them, hydrogen spillover from oxide catalyst to the zeolite surface enhances the reducibility of oxide catalysts and prevents chain growth.

To confirm these conclusions, hydrogen adsorption over the hybrid catalysts prepared through the three ways presented in Fig. 2 was used and the results are presented in Fig. 5.

Over oxide catalyst CZA, 0.8 μmol/g_{CZA} of H_2 was adsorbed; however, mixing the oxide catalyst with a zeolite induces a significant change in hydrogen adsorption over the hybrid catalysts. In fact, over the hybrid catalysts, the amount of hydrogen adsorbed increased significantly, and this feature is more pronounced when the proximity between oxide and zeolite increases, as shown in Fig. 5.

In the case of the hybrid catalyst M1, an amount of 0.3 $\mu mol \cdot g^{-1}$ was obtained, which then increases with the

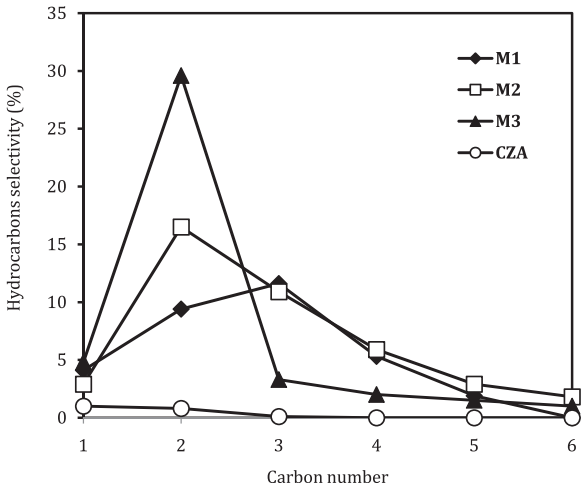

Fig. 4. Effect of the contact between oxide and zeolite on hydrocarbon selectivity.

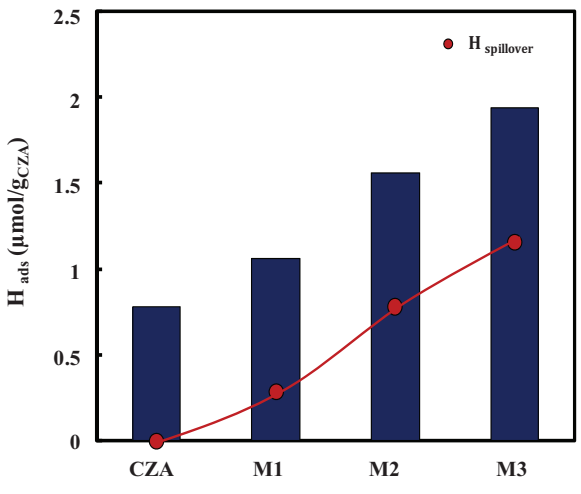

Fig. 5. (Color online.) H_2 adsorption together with $H_{spillover}$ over hybrid catalysts for M1, M2, and M3.

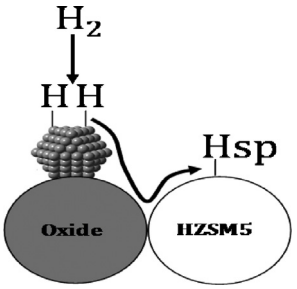

Fig. 6. Hydrogen spillover over hybrid catalysts.

increase of the proximity oxide–zeolite to reach 1.1 $\mu mol \cdot g^{-1}$ in the case of M3.

This increase is explained by hydrogen spillover (Fig. 6), and its value increases in the proximity between oxide and zeolite.

The amount of the hydrogen spillover was calculated using the following formula:

$$H_{spillover} = H_{ads}(\mu mol \cdot g_{Mi}{}^{-1}) - H_{ads}(\mu mol \cdot g_{CZA}{}^{-1}),$$
$$i = M1, M2, M3.$$

This results are in good agreement with the hydrocarbon distribution, where the higher yield of C2 is obtained with catalytic bed M3, in which hydrogen spillover is the most important; consequently, the carbon chain growth is avoided.

4. Conclusion

Hybrid catalysts prepared by physically mixing a copper-based catalyst with HZSM-5 were used for hydrocarbon synthesis through carbon dioxide hydrogenation. It was shown that the addition of HZSM-5 does not affect the copper particles size, whereas the hydrogenation of CO_2 into hydrocarbons was found to be strongly influenced by the proximity between oxide and zeolite. Indeed, the highest conversion and the best yield of hydrocarbons (mainly C_2) were obtained when the proximity between oxide and zeolite was low. The formation of C_2 is explained by hydrogen spillover, which does not promote chain growth.

Acknowledgements

H. Ahouari thanks the Institute of Chemistry of Media and Materials in Poitiers (IC2MP) and the "Agence universitaire de la Francophonie" (AUF) for financial support.

References

[1] M.J. Choi, J.S. Kim, H.K. Kim, S.B. Lee, Y. Kang, K.W. Lee, Korean J. Chem. Eng. 18 (5) (2001) 646–651.
[2] K. Fujimoto, T. Shikada, Appl. Catal. A 31 (1987) 13–23.
[3] Y.K. Park, K.C. Park, S.K. Ihm, Catal. Today 44 (1998) 165–173.
[4] J.S. Kim, S. Lee, S.B. Lee, M.J. Choi, K.W. Lee, Catal. Today 115 (2006) 228–234.
[5] T. Inui, H. Hara, T. Takeguchi, K. Ichino, J.B. Kim, S. Iwamoto, S.B. Pu, Energy Convers. Manage. 38 (1997) 385–390.
[6] S.R. Yan, K.W. Jun, J.S. Hong, M.J. Choi, K.W. Lee, Korean J. Chem. Eng. 16 (3) (1999) 357–361.
[7] S.R. Yan, K.W. Jun, J.S. Hong, M.J. Choi, K.W. Lee, Appl. Catal. A 194–195 (2000) 63–70.
[8] Y. Tan, M. Fujiwara, H. Ando, Q. Xu, Y. Souma, Indian Eng. Chem. Res. 38 (1999) 3225–3229.
[9] G. Kishan, M.W. Lee, S.S. Nam, M.J. Choi, K.W. Lee, Catal. Lett. 56 (1998) 215–219.
[10] J.S. Kim, S.B. Lee, M.J. Choi, Y. Kang, K.W. Lee, Stud. Surf. Sci. Catal. 153 (2004) 177–180.
[11] S.S. Nam, S.J. Lee, H. Kim, K.W. Jun, M.J. Choi, K.W. Lee, Energy Convers. Manage. 38 (1997) 397–402.
[12] G.C. Chinchen, P.J. Denny, J.R. Jennings, M.S. Spencer, K.C. Waugh, Appl. Catal. A 36 (1988) 1–65.
[13] J.C.J. Bart, R.P.A. Sneeden, Catal. Today 2 (1987) 1–124.
[14] T. Inui, K. Kitagawa, T. Takeguchi, T. Hagiwara, Y. Makino, Appl. Catal. A 94 (1993) 31–44.
[15] H. Arakawa, Stud. Surf. Sci. Catal. 114 (1998) 19–30.
[16] J.K. Jeon, K.E. Jeong, Y.K. Park, S.K. Ihm, Appl. Catal. A 124 (1995) 91–106.
[17] M. Fujiwara, R. Kieffer, H. Ando, Y. Souma, Appl. Catal. A 130 (1995) 105–116.
[18] E.D. Batyrev, J.C. van den Heuvel, J. Beckers, W.P.A. Jansen, H.L. Castricum, J. Catal. 229 (2005) 136–143.
[19] X. Guo, D. Mao, G. Lu, S. Wang, G. Wu, J. Catal. 271 (2010) 178–185.
[20] M. Turco, G. Bagnasco, U. Costantino, J. Catal. 228 (2004) 56–65.
[21] C. Yang, Z. Ma, N. Zha, W. Wei, T. Hu, Y. Sun, Catal. Today 115 (2006) 222–227.
[22] R. Zhou, T.M. Yu, X.Y. Jiang, F. Shen, X.M. Zheng, Appl. Surf. Sci. 148 (1999) 263–270.
[23] I.M. Caberera, M.L. Granados, J.L.G. Fierro, J. Catal. 210 (2002) 273–284.
[24] X. Zhang, L. Zhong, Q. Guo, H. Fan, H. Zheng, K. Xie, Fuel 89 (2010) 1348–1352.
[25] M. Fujiwara, R. Kieffer, H. Ando, Q. Xu, Y. Souma, Appl. Catal. A 154 (1997) 87–101.
[26] A.G. Trenco, A. Martínez, Appl. Catal. A 179 (2012) 43–51.
[27] Q. Ge, Y. Huang, F. Qiu, S. Li, Appl. Catal. A 167 (1998) 23–30.
[28] G.R. Moradi, M. Nazari, F. Yaripour, Fuel Process. Technol. 28 (2008) 1287–1296.
[29] G. Ertl, H. Knozinger, J. Weitkamp, Handbook of Heterogeneous Catalysis, vol. 3, 1997, 911–1489.
[30] H. Ahouari, A. Soualah, A. Le Valant, L. Pinard, P. Magnoux, Y. Pouilloux, React. Kinet. Mech. Catal. 110 (2013) 131–145.
[31] M. Fujiwara, R. Kieffer, H. Ando, Y. Souma, Appl. Catal. A 121 (1995) 113–124.
[32] R.V. Dmitriev, K.H. Steinberg, A.N. Detjuk, F. Hofmann, H. Bremer, K.H.M. Minachev, J. Catal. 65 (1980) 105–109.
[33] M. Sahibzada, D. Chadwick, I.S. Metcalfe, Catal. Today 29 (1996) 367–372.